Journal of Ovonic Research Vol. 16, No. 6, November - December 2020, p. 369 - 377

OPTIMIZATION OF Cu_2O AND CuSCN AS HTL OF PLANAR PEROVSKITE SOLAR CELLS VIA NUMERICAL SIMULATION

Z. KOTHANDAPANI[a], M. A. ISLAM[b,*], Y. REZA[a], ABDULWAHAB A. Q. HASAN[a], A. A. ALKAHTANI[a], N. AMIN[a,b,*]

[a]*Institute of Sustainable Energy, Universiti Tenaga Nasional (@The National Energy University), Jalan IKRAM-UNITEN, 43000 Kajang, Selangor, Malaysia*
[b]*Department of Electrical Engineering, Faculty of Engineering, University of Malaya, Jalan Universiti, 50603 Kuala Lumpur, Selangor, Malaysia*
[c]*Dept. of Electrical, Electronic and Systems Engineering, Faculty of Engineering and Built Environment, The National University of Malaysia, 43600 Bangi, Selangor, Malaysia*

Perovskite solar cells have gained a great deal of interest as it has low cost, suitable electronic and optical properties, and strong light absorption. Since the replacement of liquid electrolyte in 2012, there has been a need to optimize the Hole Transport Layer (HTL) to achieve higher efficiency. Copper Thiocyanate (CuSCN) and Cuprous Oxide (Cu_2O) are inorganic HTLs, which have a bandgap of 3.4eV and 2.17eV respectively are abundant, non-toxic, and suitable for band matching. Using CuSCN and Cu_2O as an electron blocking layer allows for reducing manufacturing cost and improving solar cell performance. Inorganic HTLs such as CuI and NiO are proven to have good stability, low cost, and high mobility. Currently, organic HTLs such as Spiro MeOTAD produce higher efficiency, however, they have poor thermal stability. This work looks into optimizing the CuSCN and Cu_2O as an HTL to replace the expensive Spiro MeOTAD, which incurs high manufacturing costs. Using SCAPS-1D software, an efficiency of 21.5% was achieved by varying the parameters of the HTL and absorber layer. The results indicate that CuSCN is a better HTL compared to Cu_2O.

(Received August 12, 2020; Accepted November 18, 2020)

Keywords: Perovskite, CuSCN, Cu_2O, HTL, Optimization, SCAPS-1D

1. Introduction

In 2017, electricity generated from renewable energy has reached up to 25% of global power. Solar power has been the obvious choice to reduce carbon emission globally and global warming. The first generation solar using silicon wafers are stable and are 80% of the commercially produced solar cells in the world. However, the cost of manufacturing and complexity are not desirable. For the second generation solar cell, thin films solar cells such as Cadmium Tellurium (CdTe), Copper Indium Gallium Selenide (CiGS), and amorphous silicon (a-Si) were created. The advantages of thin films are that they cost less and are proven to achieve higher efficiency than the first generation solar cell [1]. The third-generation solar cells like dye-sensitized solar cells (DSSCs), polymer solar cells, and perovskite solar cells have been proven to have low manufacturing cost, less complexity and are capable of reaching higher efficiency [2, 3].

Perovskite solar cells have gained much attention since Kojima *et al*. were able to achieve an efficiency of 3.8% in 2009 [4]. In 2012, Graetzel *et al.* replaced the liquid electrolyte with a solid hole transport material and achieved a PCE of 9.7% [5]. The replacement of liquid electrolyte was necessary as liquid electrolyte caused recombination and chemical instability [6]. Snaith and his team were able to achieve high efficiency of 10.9% using meso-super structured organometal lead halide perovskite which reduced fundamental losses [7]. In 2013, a further significant improvement in PCE was achieved by Snaith and his team. Using vapor deposition to deposit a compact layer of TiO_2 on the planar perovskite solar cell achieved PCE of 15.4% [8]. Perovskite

* Corresponding authors: aminul.islam@um.edu.my

solar cells, which have a bandgap of 1.5eV are cheap, abundant, and possess a high absorption coefficient. They also have a high optical extinction coefficient and multiple exciton (photoinduced electron-hole pairs) generations [9]. The chemical formula for perovskite is ABX_3 where A and B are cations and X is an anion. In this work, we use methylammonium-lead-based perovskite ($CH_3NH_3PbI_3$) as the absorber layer.

One disadvantage of $CH_3NH_3PbI_3$ is that it has poor morphology which causes instability from exposure of moisture, atmospheric oxygen, and heat [10]. To overcome this instability and leakage current, two important layers are added: Electron Transport Layer (ETL) and Hole Transport Layer (HTL). ETL is also known as the hole blocking layer, allows the electrons to move to the electrode (anode). Alternatively, HTL is known as an electron blocking layer, allows the holes to pass through the back electrode (cathode). The usual materials used for ETL are Titanium Dioxide (TiO_2), Zinc Oxide (ZnO), and Phenyl-C61-butyric acid methyl ester (PCBM). For HTL, organic and inorganic materials have been tested for suitability. Organic materials such as spiro-OMeTAD [2,2′,7,7′tetrakis(N,N-di-p-methoxyphenyl-amine)9,9′-spirobifluorene], PTAA [polymer-based poly(triarylamine)] and PEDOT:PSS [poly(3,4-ethyl-needioxythiophene): poly(styrene-sulfonate)] yields high efficiency but incurs high cost and has also stability issues as well [11,12]. Inorganic hole transport materials such as Copper Iodide (CuI), Copper Oxide (CuO), copper thiocyanate (CuSCN) and Nickel Oxide (NiO), etc. have been of great focus for their low cost and better stability under high temperature and moisture [13].

Comparing and optimizing the two inorganic materials; CuSCN and Cu_2O as HTLs are the key outcomes in this paper. Both CuSCN and Cu_2O are abundant, p-type material has high acceptor density, high mobility, and are suitable for band matching [14-16]. High bandgap materials are important to capture high energy photons. The Valence Band (VB) of perovskite should be just a little lower than the VB of HTL, which makes CuSCN and Cu_2O suitable materials [17-21]. On the other hand, the conduction band (CB) of the HTL should be higher than the CB of perovskite to avoid recombination. The schematic drawing of perovskite solar can be seen in Fig. 1.

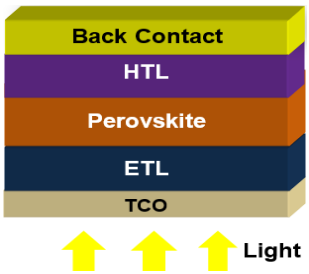

Fig. 1. Schematic drawing of perovskite solar cell investigated in this study.

2. Materials and methodology

In this work, the optimization of the perovskite solar cell is done using Solar Cell Capacitance Simulator (SCAPS). SCAPS was invented at the University of Gent, Belgium, and is used to model polycrystalline semiconductor solar cells [22, 23]. The advantage of using SCAPS is that multiple semiconductor layers can be designed and interface layers can also be inserted. SCAPS is a realistic simulation as it takes into account the bandgap, possibilities of recombination, the energy bands, etc. SCAPS simulation uses the three basic semiconductor equations: the continuity equations for holes (Eq.1) and electrons (Eq. 2) and the Poisson (Eq.3) [24].

$$\frac{dn_p}{d_t} = G_n - \frac{n_p - n_{po}}{\tau_o} + n_p\mu_n\frac{d\xi}{dx} + \mu_n\xi\frac{dn_p}{dx} + D_n\frac{d^2n_p}{dx^2} \quad (1)$$

$$\frac{dp_n}{d_t} = G_p - \frac{p_n - p_{no}}{\tau_o} + p_n\mu_p\frac{d\xi}{dx} + \mu_p\xi\frac{dp_n}{dx} + D_n\frac{d^2p_n}{dx^2} \quad (2)$$

$$\frac{d}{d_x}\left(-\varepsilon(x)\frac{d\varphi}{dx}\right) = q[p(x) - n(x) + N_D^+(x) - N_A^-(x) + p_t(x) - n_t(x)] \quad (3)$$

where G denotes the generation rate, τ_n, and τ_p denote electron and hole lifetime respectively, μ_n and μ_p are the electron and hole mobilities, ε is the permittivity, D is the diffusion coefficient, q denotes the electron charge, **φ** is the electrostatic potential, $n(x)$, $p(x)$, $n_t(x)$, $p_t(x)$ refers to the concentration of free electrons, free holes, trapped electrons, and trapped holes, respectively. $N_D^+(x)$ and $N_A^-(x)$ refers to the ionized donor and acceptor concentrations. **ξ** denotes the electric field, and *x* is the direction along with the thickness.

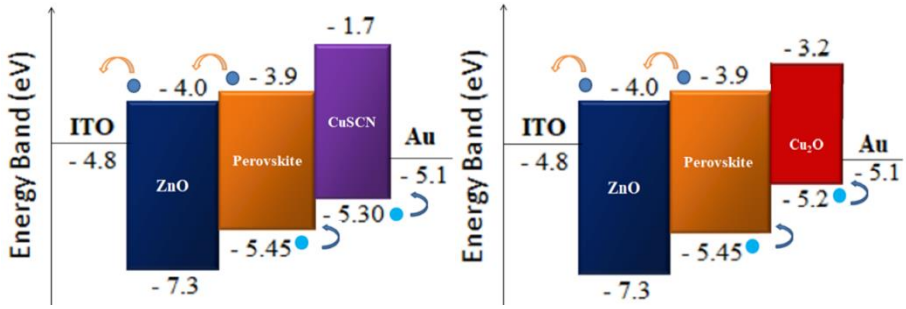

Fig. 2. Schematic band diagram of the proposed solar cells, (left) for CuSCN HTL and (right) for Cu_2O HTL.

Table 1. Input parameters for device simulation collected from the reported literature [25, 26].

	ITO	ZnO	Perovskite	CuSCN	Cu_2O
Thickness (nm)	0.2	50	800	40	20
E_g (eV)	3.5	3.3	1.5	3.4	2.17
□ (eV)	4.8	4.45	3.9	2.1	3.2
ε_r	9.0	9.00	10	10	7.110
μ_n (cm^2/Vs)	1.0E+1	1.0E+2	1.0E+1	2.0E-4	5.0E+0
μ_p (cm^2/Vs)	1.0E+1	2.5E+1	1.0E+1	1.0E-2	5.0E+0
CB DOS (cm^{-3})	5.2E+18	2.2E+18	2.2E+18	2.5E+18	2.47E+19
VB DOS (cm^{-3})	1.0E+18	1.8E+19	1.8E+19	1.8E+19	1.11E+19
N_A(cm^{-3})	0	1.0E+0	2.0E+13	1.0E+20	8.0E+13
N_D(cm^{-3})	1.0E+20	1.0E+18	0	0	0

(where E_g depicts the bandgap, Σ is the electron affinity, ε_r is the relative permittivity, μ_n and μ_p denotes mobility for electrons and holes respectively, CB DOS is the conduction band effective density of states, VB DOS is the valence band effective density of states, N_A and N_D denotes shallow uniform acceptor density and shallow uniform donor density respectively).

The Indium Tin Oxide (ITO) glass is used as the TCO in this device which acts as an anode. ITO has good optical transparency and high carrier density, which allows it to have high-level optical absorption. Zinc Oxide (ZnO) is used as the ETL because the CB of perovskite (-3.9eV) is higher than the CB of ZnO (-4.0eV) and therefore it allows for electrons to flow easily. ZnO is a suitable ETL because of its higher electron mobility and lower deposition temperature [22]. Perovskite used is a hybrid organic and inorganic, lead halide perovskite with a bandgap of

1.5eV. The VB of the HTL is important for band matching. Fig. 2 illustrates the construction of the device band structure and it can be established that VB of CuSCN and Cu_2O allows holes to transfer from perovskite. Gold (Ag) is used as the back electrode. The back-contact work function is 5.10eV (gold) and the front-contact work function is 4.4eV (ITO). In our simulation, the operating temperature is varied and the illumination spectrum is global AM1.5. The detailed parameters are tabulated in Table 1.

3. Results and discussion

Various parameters can accentuate the open-circuit voltage (V_{oc}), current density (Jsc), fill factor (FF), and PCE. In this work, the influence of the thickness of the absorber and HTL, the effect of substrate temperature, carrier concentration, and defect density were probed to optimize the performance of the device.

3.1. Influence of the Thickness of the HTLs

The thickness of HTL was varied from 20nm to 50nm. Fig.3 illustrates solar cell performance versus the thickness of HTL. It can be deduced that the V_{oc} of CuSCN is higher than of Cu_2O because the shallow acceptor of CuSCN (10^{20}) is higher compared to Cu_2O (10^{13}). The Jsc for CuSCN was highest at 40nm. For Cu_2O the Jsc drops after 40nm because of high resistance. With the highest Jsc achieved at 40nm, it can also be seen that the highest PCE of 21.05% was achieved as well. Inferring from the outcome, high PCE is caused by the increase of photons absorbed in the layer. For Cu_2O the increase in thickness decreases the PCE as well as the fill factor. The FF of CuSCN shows insignificant variation. The highest PCE for Cu_2O was obtained at 20nm.

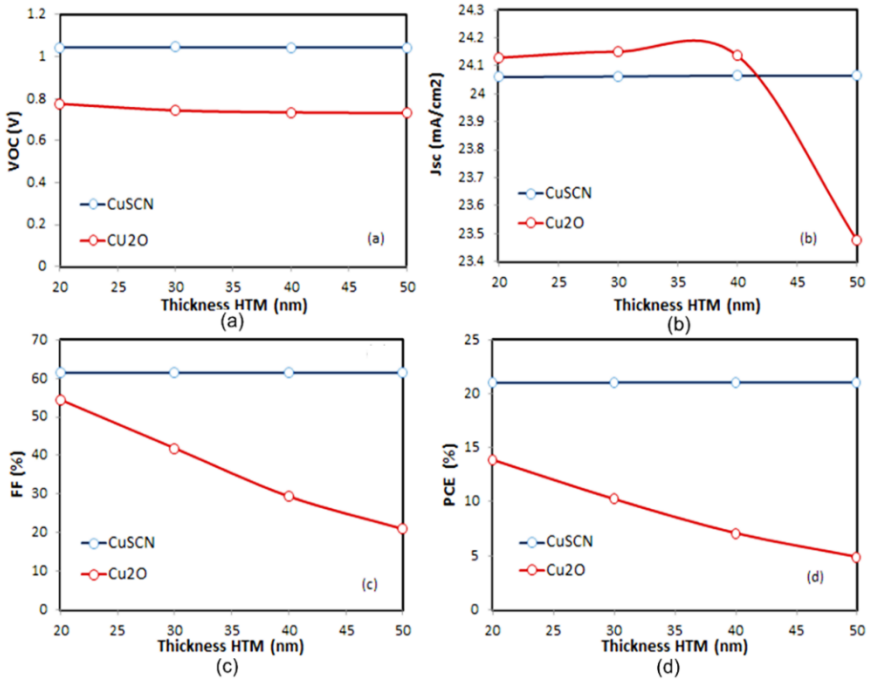

Fig. 3. Solar Cell Performance versus Thickness of HTLs; (a) Voc, (b) Jsc, (c) FF and (d) for efficiency.

3.2. Influence of the Thickness of the Perovskite layer

The thickness of the perovskite profoundly influences device performance. The variation of the thickness layer is altered from 400nm to 800nm. The increase in thickness can be complex and subjective. Fig. 4 shows the solar cell performance versus the thickness of the perovskite. It

could be seen that for both CuSCN and Cu_2O, the highest current density was achieved at a thickness of 800nm. The aforementioned simulation results are caused by the large absorption coefficient of the absorber layer. It can also be seen that the J_{SC}, as well as PCE of both Cu_2O and CuSCN, increases as the thickness of the absorber layer increases. Since the absorber thickness is less than the diffusion length of the carriers, most of the holes can reach the cathode to generate power, which leads to higher efficiency. In comparison, the FF of CuSCN minutely increases over higher perovskite thickness and CuSCN always maintained higher PCE than Cu_2O.

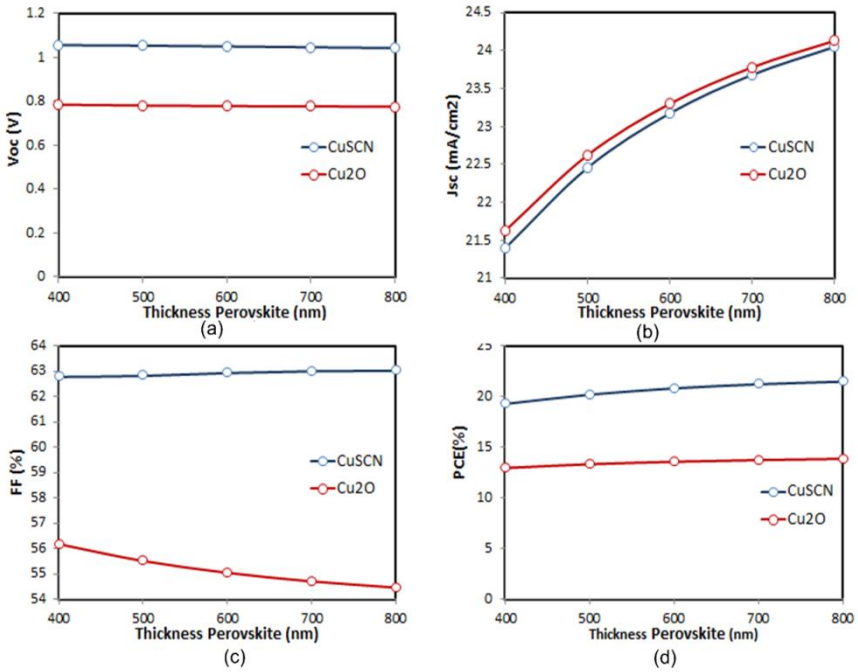

Fig. 4. Solar cell performance versus the thickness of the perovskite layer.

3.3. Influence of Defect Density in HTLs

Defect density is undesirable as it affects efficiency and stability. The defect density for the HTL Cu_2O and CuSCN has been varied from 10^{-17} till 10^{-15} cm^{-3}. The capture cross-section values used in this work is for electron and hole is 10^{-15} cm^{-3}. Results in Table 2 portray that for CuSCN, higher defect density leads to lower fill factor and therefore lower PCE values were achieved. Even though there is a decrease in solar cell performance with increasing defect density, there was not much significant change in the aforementioned results. This is because higher defect density leads to a higher recombination rate which affects the lifetime of carriers [27]. Shockley Read Hall (SRH) recombination is caused by the defect at the gap which reduces the efficiency. Interestingly, for Cu_2O, the PCE and FF remain unchanged and the cause is unknown to us.

Table 2. Influence of Defect Density for CuSCN and Cu_2O.

Defect Density (cm^{-3})	**CuSCN**			**Cu_2O**		
	Voc (V)	FF (%)	PCE (%)	Voc (V)	FF (%)	PCE (%)
10^{-17}	1.045	63.03	21.30	0.775	54.47	13.88
10^{-16}	1.045	63.02	21.29	0.775	54.47	13.88
10^{-15}	1.044	61.49	21.05	0.775	54.47	13.88

3.4. Influence of Temperature

The working temperature in SCAPS for all the above analysis has been set to 300K. To find out the temperature effect on device performance for these two device structures, the temperature was varied ranging from 350K to 410K. Certainly, the operating temperature has a significant effect on the performance of the solar cell that also observed in this study as shown in Table 3. V_{OC} is highly impacted by the increase in temperature. The decrease in V_{oc} by the increase in temperature observed in this study is caused by the increase of reverse saturation current [28]. It should be noticed that the increase in reverse saturation current limits the majority charge carrier to diffuse through the junction. The mobility is thermally activated when the temperature increases. With higher mobility, there is an increase in the fill factor. This could be caused by the tunneling of electrons and holes [29].

Table 3. Influence of temperature for CuSCN and Cu_2O.

Temperature (K)	**CuSCN**			**Cu_2O**		
	Voc (V)	FF (%)	PCE (%)	Voc (V)	FF (%)	PCE (%)
350	1.044	61.49	21.05	0.777	54.77	13.99
370	1.009	62.09	20.54	0.747	57.39	14.09
390	0.973	62.14	19.82	0.720	59.96	14.19
410	0.937	61.71	18.95	0.693	62.55	14.27

3.5. Influence of Carrier Concentration

To achieve a high current density and fill factor, a high carrier concentration is needed. Carrier concentration reflects the conductivity of the material. Low bandgap leads to higher conductivity which is essential in solar cells. The diffusion length increases with the increase of hole carriers. For CuSCN, the PCE increase drastically from 14% to 21% with the increase of carrier concentration. The FF also increases with higher carrier concentration. However, the V_{oc} minutely decreases with the increase of concentration for CuSCN but increases for Cu_2O. Table 4 denotes the influence of carrier concentration on the optoelectrical properties. The range of carrier concentration is depended on the shallow acceptor density taken from previous research [26].

Table 4. Influence of Carrier Concentration on Device.

CuSCN				**Cu_2O**			
Carrier Concentration (cm^{-3})	**Voc (V)**	**FF (%)**	**PCE (%)**	**Carrier Concentration (cm^{-3})**	**Voc (V)**	**FF (%)**	**PCE (%)**
10^{18}	1.044	61.49	21.05	**10^{13}**	0.78	54.47	13.88
10^{19}	1.042	62.64	21.38	**10^{14}**	0.78	54.49	13.89
10^{20}	1.042	63.03	21.50	**10^{15}**	0.78	54.77	13.99

3.6. Best Cell Characteristics

Sunlight emits infrared, visible, and ultraviolet rays. Quantum efficiency is used to measure the photons absorbed in the solar cell at a specific wavelength. A solar cell usually uses visible and half of the infrared wavelength. Fig. 5 illustrates the quantum efficiency of the champion cell for both CuSCN and Cu_2O. The photons are absorbed in wavelength of 400nm till 800nm which implies that the visible range and the infrared range are absorbed in the champion cell. Therefore, it could be elucidated that both Cu_2O and CuSCN HTLs are competent materials that can absorb the necessary wavelengths.

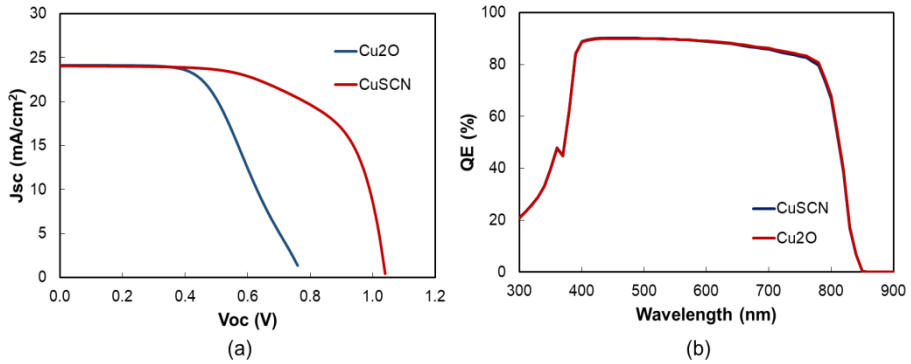

Fig. 5. (a) J-V curves and (b) Quantum efficiency of the champion solar cell for CuSCN and Cu_2O.

Champion solar cell for CuSCN was achieved with the thickness of HTL of 40nm, the thickness of Perovskite at 800nm, the carrier concentration of 10^{20}, the defect density of 10^{-17} at working point temperature of 350K. For Cu_2O, the highest PCE was achieved at thickness HTL of 20nm, the thickness of Perovskite at 800nm, carrier concentration at 10^{15}, the defect density of 10^{-17} at the working point temperature above 350K. Figure 6 indicates the I-V curve for both CuSCN and Cu_2O champion cells.

4. Conclusion

In our work, the comparison is done between Cu_2O and CuSCN as HTLs to optimize the perovskite solar cell using SCAPS simulation. To optimize the solar cell using simulation helps predict the experimental outcomes. Various parameters such as the thickness of absorber, the thickness of the HTL carrier concentration, defect density, and temperature influence the solar cell parameters. Highest PCE could be achieved using an absorber thickness of 800nm and an HTL thickness of 20nm for Cu_2O and 50nm for CuSCN. Perovskite thickness of 800nm leads to more photons absorbed and therefore higher Jsc was achieved.

To optimize the perovskite solar cell, the highest PCE for CuSCN was achieved at 350K whereas, for Cu_2O, the highest PCE was achieved at 410K. The carrier concentration of 10^{20} for CuSCN and 10^{15} for Cu_2O leads to the best solar cell performance. It could be seen that using Cu_2O as HTL has lower PCE (14%) compared to CuSCN (21%). However, the improvement of PCE and FF with an increase of temperature up to 410K indicates the assumption of higher stability compared to CuSCN. Cu_2O also had lower V_{oc} which indicates that there were more recombination losses.

Acknowledgments

The authors would like to acknowledge and appreciate the support of the Malaysian ministry of higher education for funding this work under the FRGS grant (20180113FRGS & 20190113FRGS). The authors also acknowledge the support from Universiti Tenaga Nasional under BOLD2025 grants.

References

[1] S. Sharma, K. K. Jain, and A. Sharma, Solar cells: in research and applications—a review, Materials Sciences and Applications, 6(12) (2015) 1145-1155.

[2] M. Kus, T. Y. Alic, C. Kirbiyik, C. Baslak, K. Kara and D. A. Kara, Synthesis of Nanoparticles, Handbook of Nanomaterials for Industrial Applications (24) 392-429.
[3] J. H. Noh, S. H. Im, J. H. Heo, T. N. Mandal and S. Il Seo, Chemical Management for Colorful, Efficient, and Stable Inorganic–Organic Hybrid Nanostructured Solar Cells, Nano Letters 13(4) (2013) 1764–1769.
[4] A. Kojima , K. Teshima, Y.Shirai and T. Miyasaka, Organometal Halide Perovskites as Visible-Light Sensitizers for Photovoltaic Cells, Journal of the American Chemical Society, 131(17) (2009) 6050–6051.
[5] W. Yin, L. Pan, T. Yang and Y. Liang, Recent Advances in Interface Engineering of Planar Heterojunction Perovskite Solar Cells, Molecules, 21 (7) (2016).
[6] H-S. Kim, C-R Lee, J-H Im, K-B Lee, T. Moehl, A. Marchioro, R.H-Baker, J-H Yum, J.E. Moser, M.Gratzel and N-G Park, Lead Iodide Perovskite Sensitized All-Solid-State Submicron Thin Film Mesoscopic Solar Cell with Efficiency Exceeding 9%, Nanophotonics Optical Materials and Devices Inorganic Chemistry Applied Physics (2012) 1-7.
[7] M.M. Lee, J. Teuscher, T. Miyasaka, T.N. Murakami and H.J. Snaith, Efficient Hybrid Solar Cells based on meso superstructured organometal halide perovskites, Science 338 (6107) (2012).
[8] M. Liu, M.B. Johnston and H.J. Snaith, Efficient Planar Heterojunction perovskite solar cells by vapor deposition, Nature 51 (2013).
[9] J.H.Im, C.R.Lee, J.W. Lee, S.W. Park and N.G. Park, 6.5% efficient perovskite quantum-dot-sensitized solar cell, Nanoscale, 3(10) (2011) 4088.
[10] R.Singh, P.K. Singh, B.Bhattacharya and H.W. Rhee, Review of current progress in inorganic hole transport materials for perovskite solar cells, Applied Materials Today 14 (2019) 175-200.
[11] B. A. Nejand, V. Ahmadi, S. Gharibzadeh, H. R. Shahverdi, Cuprous Oxide as a Potential Low-Cost Hole-Transport Material for Stable Perovskite Solar Cells, ChemSusChem (9) (2016) 302-313.
[12] J. H. Heo, S. H. Im, J. H. Noh, T. N. Mandal, C. S. Lim, J. A. Chang, Y. Lee, H. J. Kim, A. Sarkar, Md. K. Nazeeruddin, M. Gratzel, S.II. Seok, Efficient inorganic–organic hybrid heterojunction solar cells containing perovskite compound and polymeric hole conductors, Nature Photonics, 7(6) (2013) 486–49.
[13] J. Chen and N. G. Park, Inorganic Hole Transporting Materials for Stable and High Efficiency Perovskite Solar Cells, J. Phys. Chem. C, 122 (25) (2018) 14039-14063.
[14] N. Arora, M.I. Dar, A. Hinderhofer, N. Pellet, F. Schreiber, S.M. Zakeeruddin and M.Grätzel, Perovskite solar cells with CuSCN hole extraction layers yield stabilized efficiencies greater than 20%, Science, 358(6364) (2017)768–771.
[15] B.A. Nejand et al, Cuprous Oxide as a Potential Low-Cost Hole-Transport Material for Stable Perovskite Solar Cells, Chemsuschem 9 (2016) 302-313.
[16] B. K. H. Al-Maiyaly, B. H. Hussein, and H. K. Hassun, Growth and optoelectronic properties of p-CuO:Al/n-Si heterojunction, Journal of Ovonic Research, 16(5) (2020) 267-271.
[17] S. S. Mali, J. V. Patil, H. Kim, R. Luque, C. K. Hong, Highly efficient thermally stable perovskite solar cells via Cs:NiOx/CuSCN double-inorganic hole extraction layer interface engineering, Materials Today (26) (2019).
[18] T. H. Chowdhury, Md. Akhtaruzzaman, Md. E. Kayesha , R. Kanekoa, Ti Nodaa , J.J. Lee, A. Islam, Low temperature processed inverted planar perovskite solar cells by r-GO/CuSCN hole-transport bilayer with improved stability", Solar Energy (171) (2018) 652-657.
[19] N. N. Shlenskaya, A. S. Tutantsev, N. A. Belich, E. A. Goodilin, M. Grätzeld and A. B. Tarasov, Electrodeposition of porous CuSCN layers as hole-conducting material for perovskite solar cells, Mendeleev Communication (28) (2018) 378-380.
[20] Q. Wanga , H. Lia, J. Zhuanga, Z. Maa, F. Wanga, T. Zhanga, Y. Wang, J. Lei, Hole transport materials doped to absorber film for improving the performance of the perovskite solar cells, Materials Science in Semiconductor Processing (98) (2019) 113-120.
[21] C. Zuo and L. Ding, Solution-Processed Cu_2O and CuO as Hole Transport Materials for Efficient Perovskite Solar Cells, Small no.41(2015) 5528-5532.

[22] L.Lina, L. Jianga, P. Lia, B. Fana, Y. Qiu, A modeled perovskite solar cell structure with a Cu_2O hole-transporting layer enabling over 20% efficiency by low-cost low-temperature processing, Journal of Physics and Chemistry of Solid (124) (2019) 205-211.
[23] S. Bansal, P. Aryal, Evaluation of New Materials for Electron and Hole Transport Layers in Perovskite-Based Solar Cells Through SCAPS-1D Simulations, IEEE (2016) 747- 750.
[24] M. Burgelman, P. Nollet, S. Degrave, Modelling polycrystalline semiconductor solar cells Thin Solid Films (2000) 527-532.
[25] F,Azri, A. Meftah, N. Sengouga and A.Meftah, Electron and hole transport layers optimization by numerical simulation of a perovskite solar cell, Solar Energy 181 (2018) 372-378.
[26] S. Mahjabin, M. M. Haque, K. Sobayel, M. S. Jamal, M. A. Islam, V. Selvanathan, Abdulaziz K. Assaifan, H. F. Alharbi, K. Sopian, N. Amin, and M. Akhtaruzzaman, Perceiving of Defect Tolerance in Perovskite Absorber Layer for Efficient Perovskite Solar Cell, IEEE Access 8 (2020) 106346-106353.
[27] M.S. Jamal, S.A. Shahahmadi, P. Chelvanathan, N. Asim, H. Misran, M.I. Hossain, N. Amin, K. Sopian, Md. Akhtaruzzaman, Effect of Defect Density and Energy Level Mismatch on the Performance of Perovskite Solar Cells by Numerical Simulation, Optik (2018).
[28] A.D. Pogrebnjak, A.K.M. Muhammed, Simulation Study Of Effects, Operating Temperature And Layer Thickness On Thin Film Cigs Solar Cell Performance, J. Nano- Electron. Phys. 3(4) (2011) 51-58.
[29] J.C. Hummelen, Z. Chiguvare, M. Knipper and D. Chirvase, Temperature dependent characteristics of poly (3 hexylthiophene)-fullerene based heterojunction organic solar cells", Journal of Applied Physics 93 (3376) (2003).